INFRASOUND OBSERVATIONS FROM THE SOURCE PHYSICS EXPERIMENT (TESTS 1 AND 2) AT THE NEVADA NATIONAL SECURITY SITE

Kyle R. Jones[1], Rod W. Whitaker[2], and Stephen J. Arrowsmith[2]

Sandia National Laboratory[1] and Los Alamos National Laboratory[2]

Sponsored by the National Nuclear Security Administration

Award No. DE-AC52-06NA25946/NST11-NCNS-TM-EXP-PD15

ABSTRACT

The overall mission of the National Center for Nuclear Security (NCNS) Source Physics Experiment (SPE-N) at the Nevada National Security Site (NNSS) near Las Vegas, Nevada is to improve upon and develop new physics based models for underground nuclear explosions using scaled, underground chemical explosions as proxies. Infrasound has been used for many years to study explosive sources both above and below ground. For most of these studies, the explosions were single shot events located in different areas. With the SPE-N series of explosions, we have the unique and rare opportunity to study infrasound generated by a well-characterized source from the same borehole. This reduces the number of variables that must be accounted for when generating models using the acoustic data. At the time of submission, the first two explosive tests (SPE-N-1 and SPE-N-2) were successfully conducted on May 3 and October 25, 2011, respectively. SPE-N-1 had a yield of 0.1 tons at a depth of 60 m with a scaled depth of burial of 1,026 m. This explosion was used as a calibration shot as it was the first in the series. SPE-N-2 had a yield of 1 ton at a depth of 45 m, corresponding to a scaled depth of burial of 357 m. The acoustic amplitudes ranged from ~0.5 Pa at 225 m, to not being detected after 1 km for the 0.1 ton shot; and ~14 Pa at 225 m, to ~0.1 Pa at 5 km for the 1 ton shot. This paper will focus on detailed acoustic observations from both of these tests as well as describe future work, including detailed modeling of infrasound generation at the surface in the area above the explosion.

Report Documentation Page

Form Approved
OMB No. 0704-0188

1. REPORT DATE **SEP 2012**	2. REPORT TYPE	3. DATES COVERED **00-00-2012 to 00-00-2012**

4. TITLE AND SUBTITLE **Infrasound Observations from the Source Physics Experiment (Tests 1 and 2) at the Nevada National Security Site**	5a. CONTRACT NUMBER 5b. GRANT NUMBER 5c. PROGRAM ELEMENT NUMBER
6. AUTHOR(S)	5d. PROJECT NUMBER 5e. TASK NUMBER 5f. WORK UNIT NUMBER
7. PERFORMING ORGANIZATION NAME(S) AND ADDRESS(ES) **Los Alamos National Laboratory,P.O. Box 1663 ,Los Alamos,NM,87545**	8. PERFORMING ORGANIZATION REPORT NUMBER
9. SPONSORING/MONITORING AGENCY NAME(S) AND ADDRESS(ES)	10. SPONSOR/MONITOR'S ACRONYM(S) 11. SPONSOR/MONITOR'S REPORT NUMBER(S)

12. DISTRIBUTION/AVAILABILITY STATEMENT

Approved for public release; distribution unlimited

13. SUPPLEMENTARY NOTES

Published in the Proceedings of the 2012 Monitoring Research Review - Ground-Based Nuclear Explosion Monitoring Technologies, 18-20 September 2012, Albuquerque, NM. Volume II. Sponsored by the Air Force Research Laboratory (AFRL) and the National Nuclear Security Administration (NNSA). U.S. Government or Federal Rights License

14. ABSTRACT

The overall mission of the National Center for Nuclear Security (NCNS) Source Physics Experiment (SPE-N) at the Nevada National Security Site (NNSS) near Las Vegas, Nevada is to improve upon and develop new physics based models for underground nuclear explosions using scaled, underground chemical explosions as proxies. Infrasound has been used for many years to study explosive sources both above and below ground. For most of these studies the explosions were single shot events located in different areas. With the SPE-N series of explosions, we have the unique and rare opportunity to study infrasound generated by a well-characterized source from the same borehole. This reduces the number of variables that must be accounted for when generating models using the acoustic data. At the time of submission, the first two explosive tests (SPE-N-1 and SPE-N-2) were successfully conducted on May 3 and October 25, 2011, respectively. SPE-N-1 had a yield of 0.1 tons at a depth of 60 m with a scaled depth of burial of 1,026 m. This explosion was used as a calibration shot as it was the first in the series. SPE-N-2 had a yield of 1 ton at a depth of 45 m, corresponding to a scaled depth of burial of 357 m. The acoustic amplitudes ranged from ~0.5 Pa at 225 m, to not being detected after 1 km for the 0.1 ton shot; and ~14 Pa at 225 m, to ~0.1 Pa at 5 km for the 1 ton shot. This paper will focus on detailed acoustic observations from both of these tests as well as describe future work, including detailed modeling of infrasound generation at the surface in the area above the explosion.

15. SUBJECT TERMS

16. SECURITY CLASSIFICATION OF:			17. LIMITATION OF ABSTRACT	18. NUMBER OF PAGES	19a. NAME OF RESPONSIBLE PERSON
a. REPORT **unclassified**	b. ABSTRACT **unclassified**	c. THIS PAGE **unclassified**	**Same as Report (SAR)**	**10**	

Standard Form 298 (Rev. 8-98)
Prescribed by ANSI Std Z39-18

OBJECTIVES

The objective of this research is to use the SPE-N at the NNSS to study infrasound generated by underground explosions that occur at a well-characterized site. A primary goal of the project is to produce physics-based models to better understand and analyze explosive sources both above and belowground. At the time of submission, the first two explosive tests (SPE-N-1 and SPE-N-2) were successfully conducted on May 3 and October 25, 2011, respectively. This paper will focus on detailed acoustic observations from both of these tests as well as describe future work, including modeling of infrasound generation at the surface in the region above the explosion.

RESEARCH ACCOMPLISHED

Background

We will discuss infrasound data collected during the first two underground explosions conducted for the SPE-N at the NNSS. These series of explosions are intended such that only one variable is changed at a time, so that the data from each shot can be analyzed for subtle differences stemming from these changes. The first seven explosions will occur in “simple” granite geology at the same location as the previous nuclear experiments Hard Hat (5.7 kt; 2/15/1962) and Pile Driver (62 kt; 6/2/1966) (DOE/NV-209, 1994). Several more shots will be conducted in a “complex” geologic setting (yet to be determined). For each series (simple and complex) we will re-occupy our station and sensor locations for each subsequent explosion. It is important to note that the primary purpose of the source physics experiment is to study the seismic waves generated from explosions in both damaged and undamaged rock and that the observed infrasound is a fortuitous side effect of those explosions.

Infrasound, while not the primary goal, is still an important component to the SPE-N series of experiments because infrasound signals can still be detected, even though there is little visible surface expression of the shots. The data can be analyzed to determine yield, extent of the surface expression (spall), and energy coupled to the atmosphere. With the ground truth information available from these experiments, we will be able to further our understanding of the previously developed empirical relationships among shot size, emplacement depth and source area to evaluate what factors affect infrasound generation from underground explosions.

The IML-ST infrasound sensor, manufactured by Inter-Mountain Labs, was used for both of the first two tests. This sensor has an approximately flat response between 2 and 30 Hz with a sensitivity of 0.20 Volts/Pa (http://www.intermountainlabs.com/pdf/IML_ModelSTDataSheet.pdf). The Sandia National Laboratory Facility for Acceptance, Calibration and Testing (FACT) Site conducted an independent and detailed evaluation/characterization of this sensor (Hart, 2007). The primary purpose of the IML sensor (model SS) is to detect avalanches (Comey and Mendnhall, 2004) but has been redesigned (model ST) to study different infrasound sources, from earthquakes to explosions (Stump et al., 2007; Hale et al., 2010). The IML contains 20 small electret condenser microphones that are summed to produce an improved signal-to-noise output signal. Depending on the model, either four or eight hose connector ports are used to attach porous hoses for wind noise reduction. The output from the sensors was digitized on a Reftek RT-130 digitizer set to a gain of 32 with a sampling rate of 500 samples per second (500 Hz).

For the first two experiments, seven stations were distributed azimuthally about ground zero at ~230 m with stations extending Southeast at distances of 1, 2 and 5 km (Figure 1). Each station had five IML-ST infrasound sensors. Four sensors had 50 ft. porous hoses for wind reduction and one sensor was left open to the elements. They were arranged in a roughly triangular geometry with one sensor North, two Southeast and Southwest, respectively, and two in the center. Each leg is approximately 30 m away from center. One of the center sensors was the one without porous hoses and was approximately co-located with the center sensor. For this paper, only data recorded at the sensors with the wind reductions systems will be discussed. All figures, except where noted, were produced with data that have been broadband filtered between 1 and 10 Hz using a four-pole Butterworth filter.

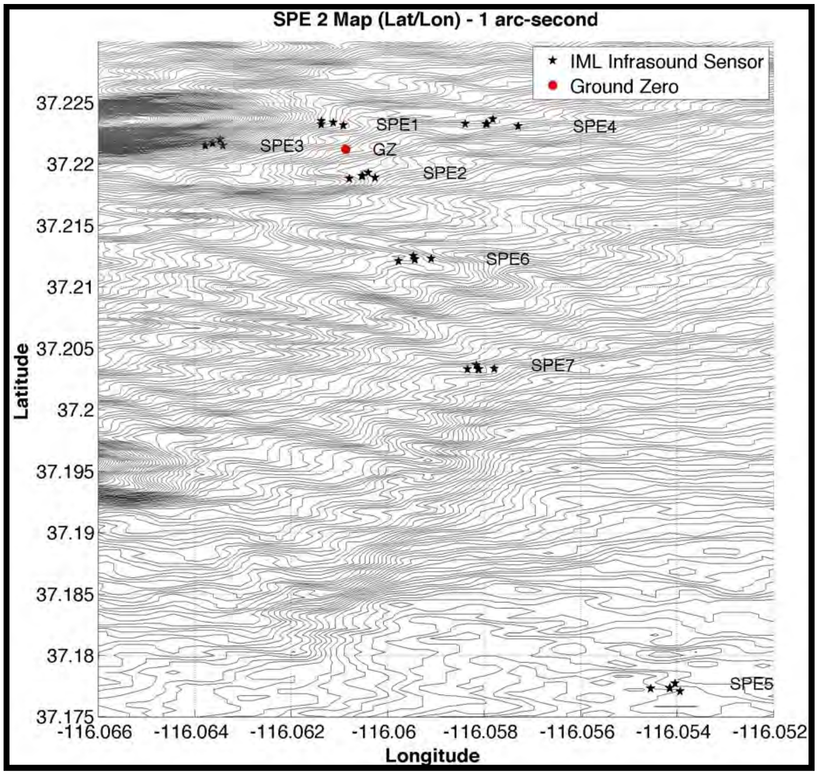

Figure 1. Topographic map showing each infrasound sensor (black star) at the seven SPE-N station locations and ground zero (red circle). The station locations remained the same for SPE-N-1 and SPE-N-2.

SPE-N Shot 1

The first explosion, conducted May 3, 2011, at 22:00:00 UTC, had a yield of 0.1 tons at 60 m depth of burial (DOB), corresponding to a scaled depth of burial (SDOB) of 1,026 m. This first explosion was designed to be a calibration shot to determine, empirically, the Green's functions for the surrounding rock. The shot plan called for a line of Det-Cord to be emplaced from the working point to the surface, as a secondary means of detonation should the electronic detonation fail. The Det-Cord was wrapped around several sandbags at the surface, above the hole and again buried with more sandbags. During the shot, the primary electronic detonator worked as planned and set off the Sensitized Heavy Ammonium Nitrite and Fuel Oil (SHANFO). This in turn ignited the Det-Cord resulting in an explosion at the surface. After the Det-Cord exploded, the weld on a line-of-sight pipe, that goes from the working point to the surface, failed and ejected out of the hole. A review of the acoustic data show that there was little to no significant acoustic energy released into the atmosphere, at least not sufficient enough to interfere with the detection of the primary explosion. In this case, the dominant source of the infrasound is the vertical ground motion from the detonation of the SHANFO with an estimated spall size of ~50 m in diameter. However, even with the stemming failure, the observed amplitudes for this shot are very low due to the yield (<<1 Pa at the closest station – Table 1), compared to the ~14 Pa observed for SPE-N-2 (Table 2).

Table 1. Station number, mean peak amplitude (Pa) (i.e. peak amplitudes from all sensors at each station are averaged) and mean distance (km). Note – the stations have been ordered according to distance. The amplitudes marked with a (*) are noise estimates since the signal-to-noise is too low to measure an amplitude of the signal.

Station	Mean Peak Amplitude (Pa)	Mean Distance (km)
1	0.30	0.24
2	0.35	0.25
3	0.41	0.25
4	0.23	0.35
6	0.13*	0.99
7	0.07*	2
5	0.10*	5

For this shot, only the four closest stations (0.25 km) recorded the explosion with decent signal-to-noise ratios. The station located at 1 km recorded the signal but with a much reduced amplitude, while the two farthest stations, 2 and 5 km respectively, did not record the shot with sufficient signal strength. We normalized and cross-correlated each recorded signal with the observed signal from station 1, sensor 1 and stacked and summed the results (Figure 2A). It is clear that only the closest stations provide any benefit to the stacking. The preceding seismic signal is shown on the plot occurring at 60 seconds followed by a clear acoustic pulse. This can also be seen in detail in Figure 2B. The "m" shape of the pulse is a result of filtering and the propagation of the signal being recorded off-axis to the movement of the distributed source region.

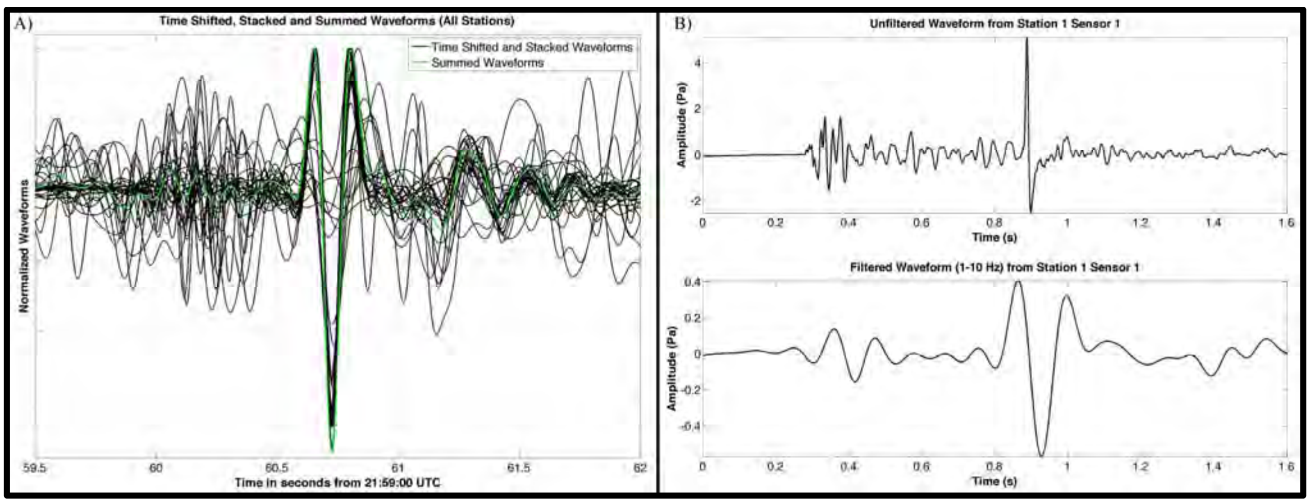

Figure 2. A) Time shifted, stacked (black) and summed (green) waveforms from all SPE-N-2 infrasound sensors. The variability in the waveforms around 60 seconds corresponds to the seismic component of the explosion signal recorded with the infrasound sensors. The rest of the variability comes from low signal-to-noise for the stations 1 km and beyond. B) Waveforms from sensor 1, station 1 shown unfiltered (top) and filtered (bottom) between 1 and 10 Hz using a 4-pole, Butterworth filter.

As shown above, the explosion was not large enough for the acoustic wave to propagate to the entire network. The waveforms from the four closest stations show the seismic signal followed by the acoustic pulse, but significantly decays to the point of not being detected at all past 1 km (Figure 3).

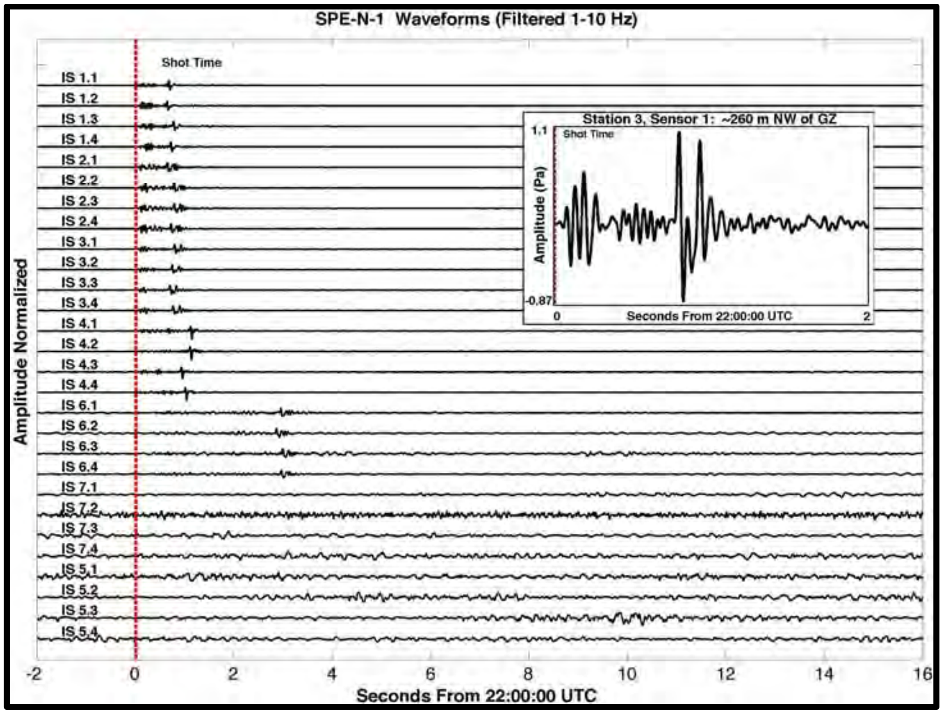

Figure 3. Normalized waveform plot showing all the infrasound sensors with an inset showing a detailed waveform from station 1, sensor 1.

For the sensors at stations 1 - 4, the close-in stations, we are able to determine if the recorded amplitudes decay according to the standard model of 1 over the distance. The American National Standards Institute (ANSI) describes the decay rate of a point source explosion to be $\frac{1}{r^{1.1}}$ (ANSI, 1983). This is to say that as distance (r) increases, the amplitude will decay at a rate of $\frac{1}{r^{1.1}}$ (Figure 4 – Red Line). This relationship generally works well for most explosions that are in the free field and directly perturbing the atmosphere. For the SPE-N series of explosions we find that since they are not in the free field, the standard model of $\frac{1}{r^{1.1}}$ doesn't fit as well as simply approximating the decay rate as $\frac{1}{r}$. Unfortunately, due to the much decreased signal-to-noise for stations 5, 6, and 7. We plot signals from only the four closest stations. Not surprisingly, the amplitudes generally fit the $\frac{1}{r}$ decay rate with some sensor variability at each station. This variability will be discussed in more detail later in the SPE-N-2 section.

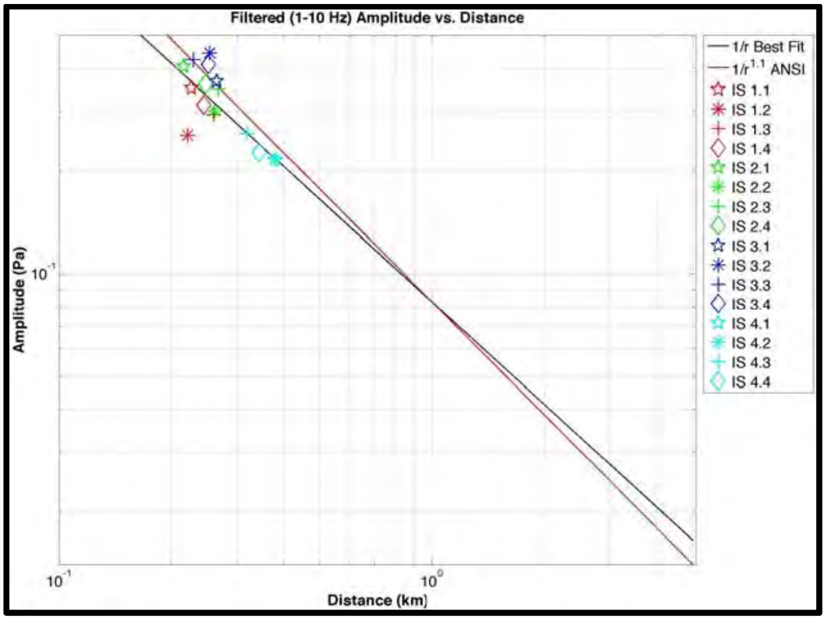

Figure 4. Amplitude vs. distance for each infrasound sensor at four of the seven stations with $\frac{1}{r}$ and ANSI $\frac{1}{r^{1.1}}$ best-fit lines. The signal-to-noise for the stations >1 km was too low to get an accurate amplitude measurement.

SPE-N Shot 2

The second explosion, conducted October 25, 2011 at 19:00:00 UTC, had a yield of 1 ton at a depth of 45 m, corresponding to a SDOB of 357 m. This shot was completely contained and resulted in a small dust cloud at the surface. The spall region was estimated to be ~90 m in diameter. The station locations and sensors were identical to those used in the SPE-N-1 experiment. The primary difference between SPE-N-1 and SPE-N-2, in terms of observed infrasound, is that all of the stations detected the SPE-N-2 explosion (Figure 6), largely due to the higher yield. The observed amplitudes ranged from ~0.2 to 13.4 Pa (Table 2).

Table 2. Station number, mean peak amplitude (Pa) (i.e., peak amplitudes from all sensors at each station are averaged) and mean distance (km). Note – the stations have been ordered according to distance.

Station	Mean Peak Amplitude (Pa)	Mean Distance (km)
1	7.68	0.24
2	10.05	0.25
3	13.44	0.25
4	6.83	0.35
6	2.01	0.99
7	0.77	2
5	0.20	5

Since SPE-N-2 had a much larger signal-to-noise ratio for the event, the resulting signal correlation, summation and stack of the recorded signals resulted in a much cleaner signal (Figure 5A). Again, preceding the event, the seismic signal is observed followed by the acoustic "N-wave" (Figure 5B). There is some variability between waveforms from each sensor, which could be related to propagation, but overall, the acoustic portion of the waveform is very similar.

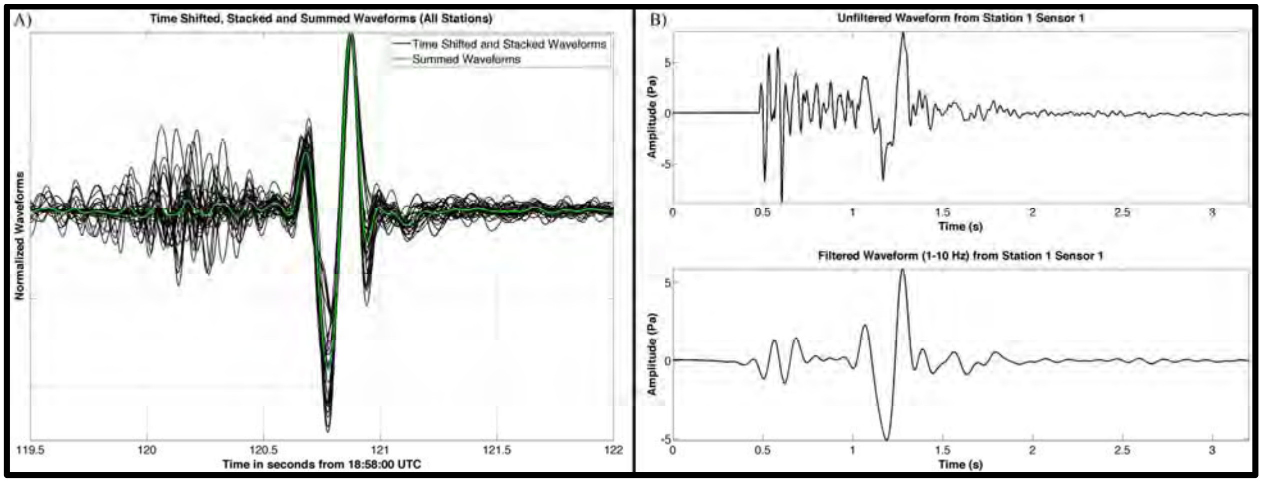

Figure 5. A) Time shifted, stacked (black) and summed (green) waveforms from all SPE-N-2 infrasound sensors. The variability in the waveforms around 120 seconds corresponds to the seismic component of the explosion signal recorded with the infrasound sensors, followed by the acoustic arrival ("N" wave). B) Waveforms from sensor 1, station 1 shown unfiltered (top) and filtered (bottom) between 1 and 10 Hz using a 4-pole, Butterworth filter.

The acoustic pressure wave from the explosion propagated across the entire network and to each sensor with the potential to have been detected to some distance past 5 km, though, not far, as the amplitude at 5 km was 0.2 Pa (Figure 6). The observed seismic signal is present on the closest stations (1 – 4) but starts to become less evident past 1 km.

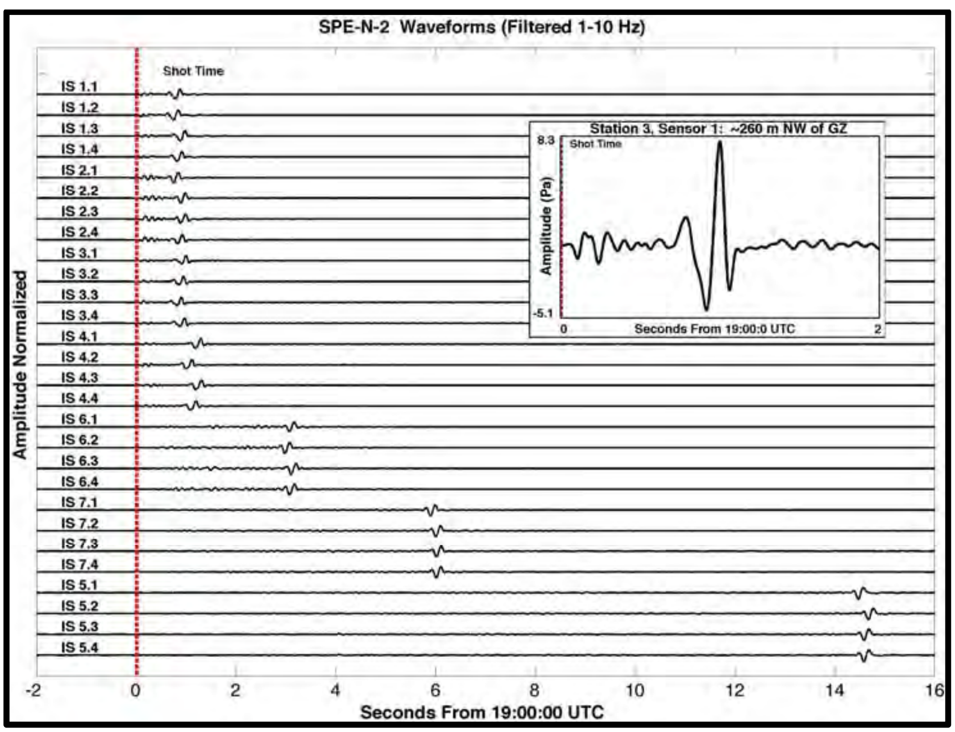

Figure 6. Normalized waveform plot showing all the infrasound sensors with an inset showing a detailed waveform from station 1, sensor 1.

As with SPE-N-1, we are able to determine the amplitude decay rate. SPE-N-2 was ten times larger than SPE-N-1, resulting in the acoustic pressure wave being observed across the entire network. We were able to use every sensor

at every station to plot the amplitude versus distance decay for the entire network (Figure 7). We again plot both the $\frac{1}{r}$ best fit and the ANSI $\frac{1}{r^{1.1}}$ solutions. In this case the $\frac{1}{r}$ solution fits more of the stations than the ANSI solution, however, the ANSI solution better follows the actual trend of the data.

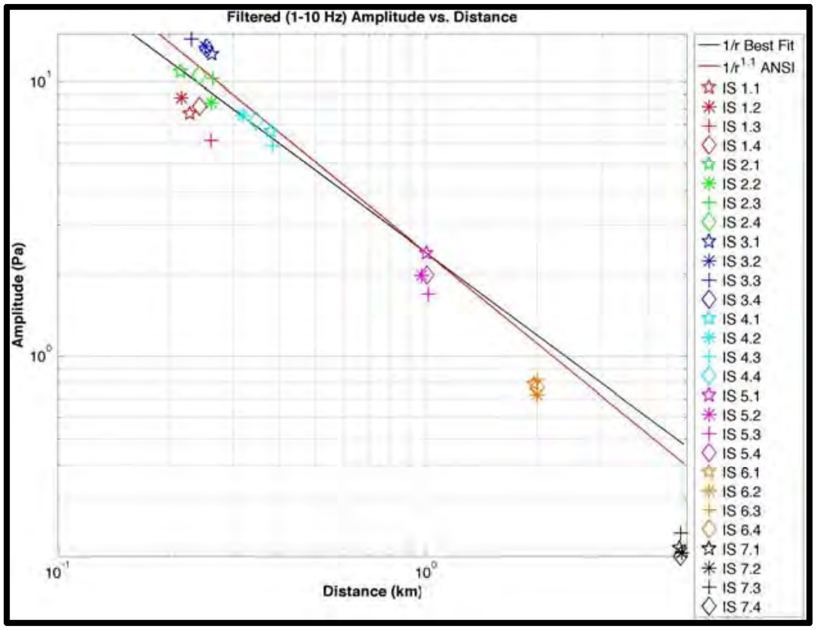

Figure 7. Amplitude vs. distance for each infrasound sensor at all seven stations with $\frac{1}{r}$ and ANSI $\frac{1}{r^{1.1}}$ best-fit lines.

There are several reasons for the variation in sensor amplitudes at each station. Wind can affect the propagation of acoustic signals (Figure 8). During the time of the shot, the wind was blowing from the Southeast to the Northwest at ~3 m/s, potentially causing the lower amplitudes observed at the more distant stations (5, 6, and 7). This may not entirely account for the variation in the near stations (1, 2, 3, and 4). In this case, it is possible that the amplitude variations are due to the placement of each sensor. Although the sensor spacing is only ~30 m, the topography is not flat in this region. This results in sensors that do not have line-of-sight (LOS) to ground zero. The sensors are also subject to some level of variability as they rely on multiple electret condenser microphones that each have their own response. The microphones are selected and the sensors are tuned to minimize this effect, but it is still a potential source of variability. Interestingly, for both SPE-N-1 and SPE-N-2, the first three stations all vary in amplitude in a similar manner; i.e., in both cases, station 3 is has a larger amplitude than station 2, and station 2 has a larger amplitude than station 1. This could potentially be caused by the topography, but future SPE-N tests are needed to further constrain the cause of the amplitude variations.

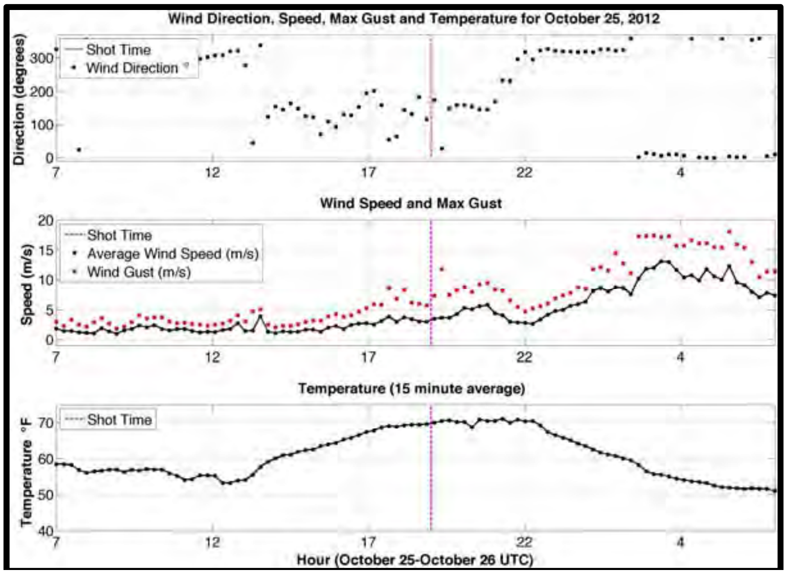

Figure 8. Onsite meteorological observations including: wind direction, wind speed, max wind gust, and temperature on a 15-minute average. The time of the shot is denoted with vertical dashed line.

Despite the sensor variability, we were able to use the infrasound sensors at each station as mini-arrays, to calculate the back azimuth to ground zero. For this analysis we use the regional infrasound monitoring software, InfraMonitor (Arrowsmith and Whitaker, 2008). Using the back azimuths (Figure 9A) from each station we use the Bayesian infrasonic source location (BISL) technique (Modrak, 2010) built into InfraMonitor to calculate a location solution. The calculated location solution agrees very well with the actual location of ground zero to within a ~35x35 m area with 95% confidence (Figure 9C).

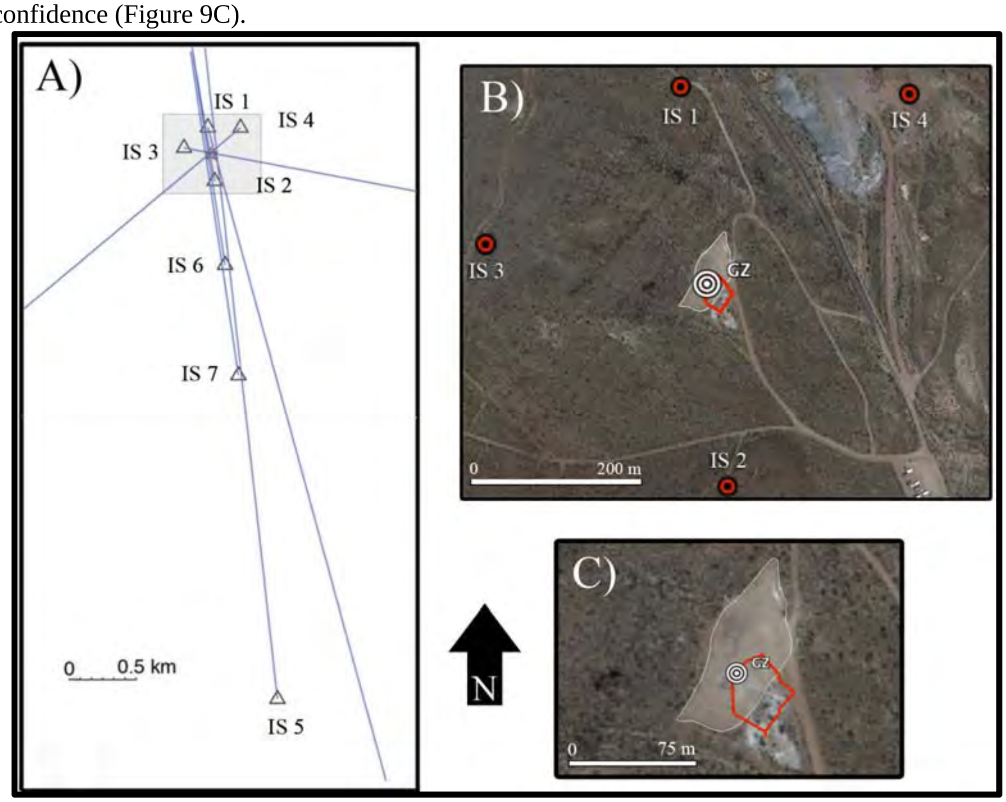

Figure 9. A) BISL location solution using the InfraMonitor detection and location software in shaded square represents enlarged area (B). B) Map of the four closest stations (1 – 4) and ground zero (white target) with a 95% confidence location solution (red). C) Close up view of the explosive pad (white), ground zero (white target) and the 95% confidence location solution (red).

CONCLUSIONS AND RECOMMENDATIONS

The explosions conducted at the NNSS, as part of the Source Physics Experiment, are invaluable to the ongoing study and understanding of infrasound generation by underground explosive events. With the level of ground truth knowledge in terms of yield, location and rock characteristics, we are able to begin to constrain specific properties of infrasound generation and propagation.

Future Work

Currently, we are working on modeling the infrasound generated from the underground explosions using several surface accelerometers located at ground zero. With the accelerometer data we can create and compare synthetic infrasound waveforms using the Rayleigh Integral Method (Whitaker, 2008; Arrowsmith et al., 2012). This will help to better understand what parameters are dominant in producing acoustic pressure waves from underground explosions.

ACKNOWLEDGEMENTS

The authors are grateful to Bobby Corbell and Chris Jones for the initial deployment and collection of the data for both shots and to Cathy Snelson, Bob White, and Ryan Emmitt for their support at NNSS.

REFERENCES

ANSI (1983). Estimating airblast characteristics for single point explosions in air with a guide to evaluation of atmospheric propagation and effects, ANSI S2.20-1983.

Arrowsmith, S. J., et al. (2012). A Seismoacoustic Study of the 2011 January 3 Circleville Earthquake. *Geophys. J. Int.* **189,** 31148–1158.

Arrowsmith, S. J. and Whitaker, R. (2008). InfraMonitor: a tool for regional infrasound monitoring, in *Proceedings of the 2008 Monitoring Research Review*: *Ground-Based Nuclear Explosion Monitoring Technologies*, LA-UR-08-05281, Vol. 2, pp. 837–843.

Comey, R. H. and Mendenhal, T. (2004). Recent studies using infrasound sensors to remotely monitor avalanche activity, in Proceedings of the 2004 International Snow Science Workshop, Jackson Hole, Wyoming.

DOE/NV-209 (1994). United States Nuclear Tests: July 1945 through September 1992. Rev. 14:p16, 26

Hale, J. M., et al. (2010). Infrasound signal characteristics from small earthquakes, in *Proceedings of the 2010 Monitoring Research Review*: *Ground-Based Nuclear Explosion Monitoring Technologies*, LA-UR-10-05578, Vol. 2, pp. 720–730.

Hart, D. M. (2007). Evaluation of inter-mountain labs infrasound sensors July 2007. Sandia National Laboratory Report, SAND2007-7020.

Inter-Mountain Labs Model ST Infrasound Sensor Datasheet. (2012) http://www.intermountainlabs.com/pdf/IML_ModelSTDataSheet.pdf

Modrak, R. T., et al. (2010). A Bayesian framework for infrasound location. *Geophys. J. Int.* **181**, 399–405.

Stump, B., et al. (2007). Seismic and infrasonic energy generation and propagation at local and regional distances: phase 1 – Divine Strake experiment, in *Proceedings of the 2007 Monitoring Research Review: Ground-Based Nuclear Explosion Monitoring Technologies,* LA-UR-07-5613, Vol. 1, pp. 674–683.

Whitaker, R., W. (2008). Infrasound signals from ground motion sources, in *Proceedings of the 2008 Monitoring Research Review: Ground-Based Nuclear Explosion Monitoring Technologies,* LA-UR-08-05281, Vol. 2, pp. 912–920.